High-Yield Preparation, Versatile Structural Modification, and Properties of Layered Cobalt Hydroxide Nanocones

Xiaohe Liu, Renzhi Ma, Yoshio Bando, and Takayoshi Sasaki*

A low-cost oil bath synthetic route is presented to produce uniform and highly crystalline layered cobalt hydroxide nanocones (NCs) intercalated with dodecyl sulfate anions ($C_{12}H_{25}OSO_3^-$, DS^-). A new exfoliating procedure, by gradually unravelling/unzipping these NCs through heat treatment in formamide-water binary solution, is developed to prepare unilamellar nanosheets. Moreover, the NCs can be readily modified with various inorganic or organic anions via a conventional anion-exchange process at ambient temperature. The exchanged product, for example, NO_3^-–intercalated NCs, can be more easily and rapidly transformed into cobalt oxides (e.g., Co_3O_4 and CoO) than the original DS^-–intercalated form while retaining a conical feature. Both the cobalt hydroxide NCs and exfoliated nanosheets are electrochemically redoxable, exhibiting a Faradaic pseudocapacitive behavior. The magnetic measurements further reveal both antiferromagnetic behaviors for transformed Co_3O_4 and CoO NCs. Their Néel temperature values are lower than those of bulk oxides due to finite size and geometric confinement effect. The peculiar conical feature of NCs with a hollow interior and tunable layer spacing, as well as exfoliated unilamellar nanosheets with all surface area exposed, may show promise for potential applications in electrochemical energy storage and magnetic devices.

1. Introduction

During the past few decades, layered metal hydroxides have drawn immense attention due to their distinctive compositional flexibility and anion exchangeability, promising a wide variety of practical and potential applications, for example, anion exchangers, adsorbents, catalysts, active electrode materials, magnetic resonance imaging (MRI) contrast agents, photofunctional materials, drug delivery systems, and so forth.[1] Generally, layered hydroxides adopt a lamellar or platy morphology resulting from a hexagonal in-plane symmetry.[2]

Dr. X. H. Liu, Dr. R. Ma, Prof. Y. Bando, Prof. T. Sasaki
International Center for Materials Nanoarchitectonics (WPI-MANA)
National Institute for Materials Science (NIMS)
1–1 Namiki, Tsukuba, Ibaraki 305–0044, Japan
E-mail: ma.renzhi@nims.go.jp
Dr. X. H. Liu
Department of Inorganic Materials
School of Resources Processing and Bioengineering
Central South University
Changsha, Hunan 410083, P. R. China

DOI: 10.1002/adfm.201400193

Recently, we have achieved a significant breakthrough in the preparation of unique layered transition-metal (Co, Ni, Co-Ni, etc.) hydroxide nanocones (NCs) under microwave-assisted hydrothermal conditions using either hexamethylenetetramine (HMT, $C_6H_{12}N_4$) or urea ($CO(NH_2)_2$) as hydrolysis agents and sodium dodecyl sulfate (SDS) as a surfactant and structure-directing agent.[3] These redoxable hydroxide NCs, possessing the advantages of a peculiar hollow features and large interlayer spacing, are very useful as active materials for the development of high-performance electrochemical energy storage devices.[3b] Nevertheless, the microwave-assisted synthetic protocol generally involves a special apparatus and a low yield, which is unfavorable to fulfilling the application prospects of these hydroxide NCs. Therefore, it remains an urgent research topic to develop a simple synthetic approach for producing transition-metal hydroxide NCs in large quantities and high uniformity.

On the other hand, layered metal hydroxides, including NCs, could be directly exfoliated/delaminated into unilamellar nanosheets via some soft chemical procedures, for example, mechanical shaking or ultrasonic dispersing in formamide.[3,4] The unilamellar nanosheets, typically with a thickness under one nanometer versus lateral size ranging from the submicrometer level to several micrometers, are ideal two-dimensional (2D) building blocks to fabricate multilayer nanofilms with tunable compositions and exciting functionalities based on layer-by-layer (LBL) and/or Langmuir-Blodgett (LB) molecular-scale assembling techniques.[5] Nevertheless, the exfoliating mechanism is still not well understood. The exfoliating/delaminating procedure needs to be further modified or improved to obtain well-defined hydroxide nanosheets with homogeneous thickness, as well as to provide a justifiable explanation for the exfoliation of layered hydroxides in general.

In current work, we have developed a convenient and cost-effective synthetic strategy, namely, oil bath synthesis, to prepare layered cobalt hydroxide NCs based on urea hydrolysis in the presence of anionic surfactant dodecyl sulfate (DS). The oil bath method may be regarded as one of the most facile and effective solution-based synthetic methods, which are widely used in many chemical laboratories. This synthesis results in a high yield and can be easily scaled-up, which may be of great

importance for future industrial applications. The influence of reaction temperature, duration time, and amount of surfactant on the morphology and size of layered cobalt hydroxide NCs was carefully investigated in detail. In particular, it was found that layered cobalt hydroxide NCs could be gradually exfoliated into unilamellar nanosheets in a formamide-water binary solution via heat treatment. Observation of the exfoliation stages implies a plausible unravelling scenario for the hydroxide NCs. Furthermore, interlayer DS anions of layered cobalt hydroxide NCs were readily exchangeable for various anions (e.g., Cl^-, ClO_4^-, CH_3COO^-, and NO_3^-, etc.) at ambient temperature, which offers an obvious advantage for structural and functional modifications. For example, NO_3^-–intercalated cobalt hydroxide NCs could be more readily transformed into cobalt oxides (e.g., Co_3O_4 and CoO) retaining original morphological features in comparison with the original DS^-–intercalated form. Futhermore, electrochemical characterizations suggested that a suitable combination of interlayer spacing and intercalated anionic species are required for achieving optimum electrochemical performance. Meanwhile, the magnetic properties of cobalt oxide NCs have been examined, revealing a weak antiferromagnetic interaction in Co_3O_4 NCs while a strong one in CoO NCs. Based on these discoveries, layered hydroxide NCs and their derivatives may be regarded as a new class of advanced nanomaterials ideal for further fundamental research and technological applications in various fields.

2. Results and Discussion

2.1. Synthesis and Characterization of Layered Cobalt Hydroxide NCs

Layered cobalt hydroxide NCs were synthesized via an oil bath method using $CoCl_2 \cdot 6H_2O$ as a cobalt source, urea as a hydrolysis reagent and SDS as a surfactant and structure-directing agent under a nitrogen gas atmosphere. The amounts of $CoCl_2 \cdot 6H_2O$ and urea were fixed at 5 mmol and 35 mmol, respectively. The amount of SDS was adjusted in a range of 0–25 mmol. In a typical synthesis, a green-colored product was obtained. **Figure 1**a depicts a representative scanning electron microscopy (SEM) image of the product prepared at 100 °C for 8 h using 12.5 mmol SDS. It is clearly seen that a large quantity of uniform conical structures were synthesized under such conditions. There was no apparent impurity observed other than the conical morphology. In the higher-magnification SEM image shown in Figure 1b, hollow interiors of the regular conical structures were clearly identified. Such a conical feature is also notable in the transmission electron microscopy (TEM) image displayed in Figure 1c. The NCs have an average bottom diameter of approximately 1 μm, tip diameter of about 200 nm, whereas a length up to 6 μm. The outer dimensions of as-prepared NCs under current oil bath conditions are similar, albeit somewhat thicker in wall thickness, to those previously

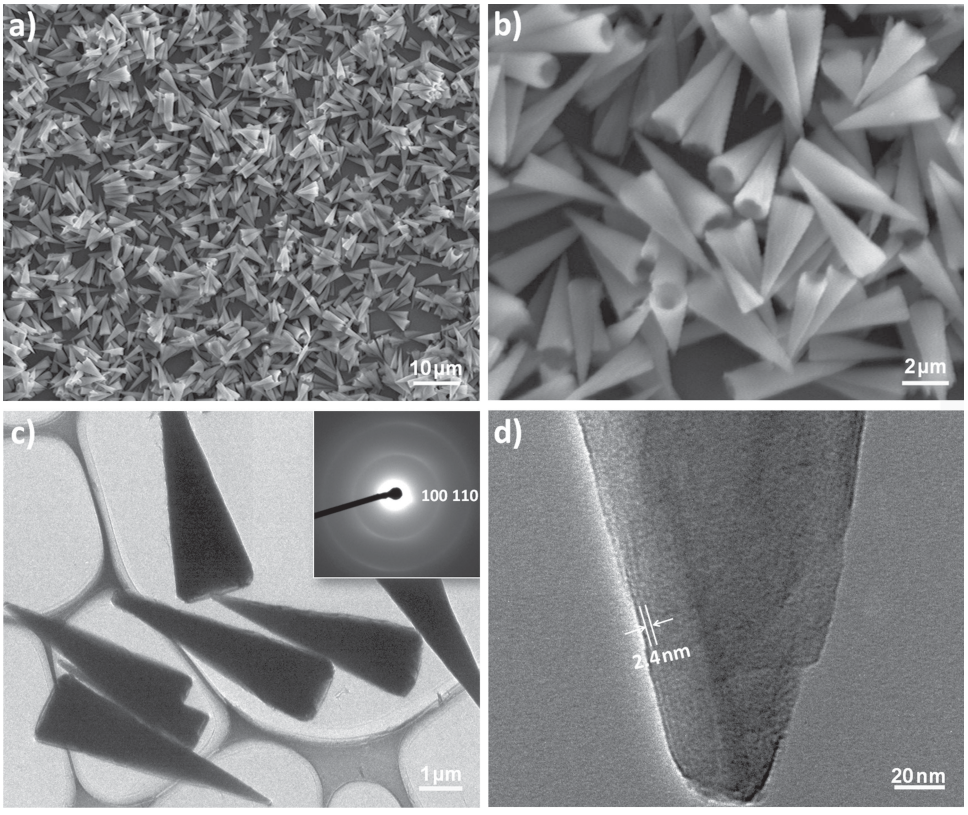

Figure 1. Oil bath synthesis of layered cobalt hydroxide NCs obtained at 100 °C for 8 h. a,b) SEM and c) TEM images. The inset in c) shows SAED pattern taken on an individual NC. d) HRTEM image of the tip part of an individual NC.

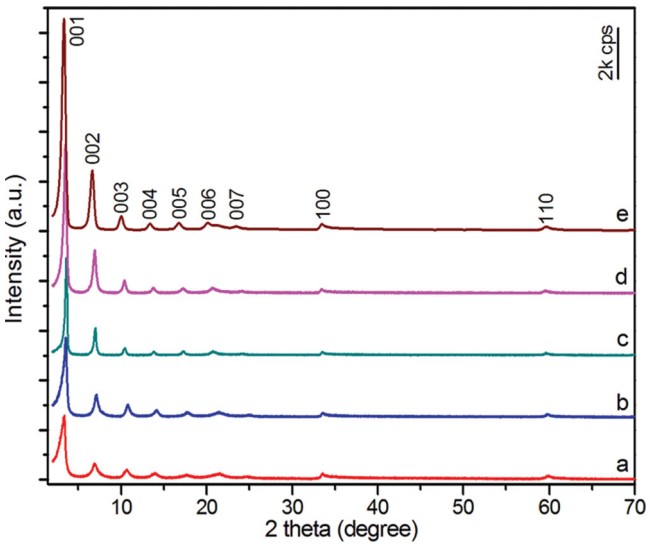

Figure 2. XRD patterns of layered cobalt hydroxide NCs obtained at 100 °C for varied time durations: a) 2 h, b) 4 h, c) 8 h, d) 12 h. e) XRD pattern of NCs obtained at 120 °C for 8 h.

obtained under microwave-assisted hydrothermal conditions also employing urea as a hydrolysis and alkaline agent.[3b] It is worth pointing out that both the outer dimensions, as well as wall thickness, are bigger than those of NCs obtained using HMT as an alkaline reagent.[3a] This might be derived from the different hydrolyzing rate of urea and HMT. Slower hydrolyzing rates of urea may be favorable for the formation of hydroxide NCs. The inset in Figure 1c represents a typical selected area electron diffraction (SAED) pattern, which can be indexed to in-plane or [001] zone-axis diffraction rings of hexagonal cobalt hydroxide with a lattice constant of a = 0.310 nm. The high-resolution TEM image of an individual cobalt hydroxide NC, as shown in Figure 1d, demonstrates a layered structure with interlayer spacing measured at about 2.4 nm, in good agreement with our previous characterizations of α-type cobalt hydroxide intercalating DS anions in the gallery.[3]

The evolution in the morphology and structure of as-prepared products was monitored by adjusting the reaction time and temperature. **Figure 2** displays X-ray powder diffraction (XRD) patterns of as-prepared products obtained at 100–120 °C for different time duration from 2 to 12 h. It is notable that the basal reflection peaks, corresponding to an interlayer spacing of about 2.4 nm, were gradually enhanced in intensity with the prolongation of the reaction time or elevation of temperature. The peaks also became sharp, implying that the crystallinity of the products was improved with a longer time or higher temperature. Such a trend was also verified in the microscopic observations. For example, when the reaction time was as short as 2 h, the product was mostly composed of small and short conical objects (**Figure 3**a). The average sizes were estimated to be approximate 3 μm in length, 100 nm in tip diameter, and 500 nm in bottom diameter. At this stage, some lamellar objects were also observed. Extending the reaction time to 4 h, almost 100% conical structures with uniform morphology were obtained, as shown in Figure 3b. The dimensions were

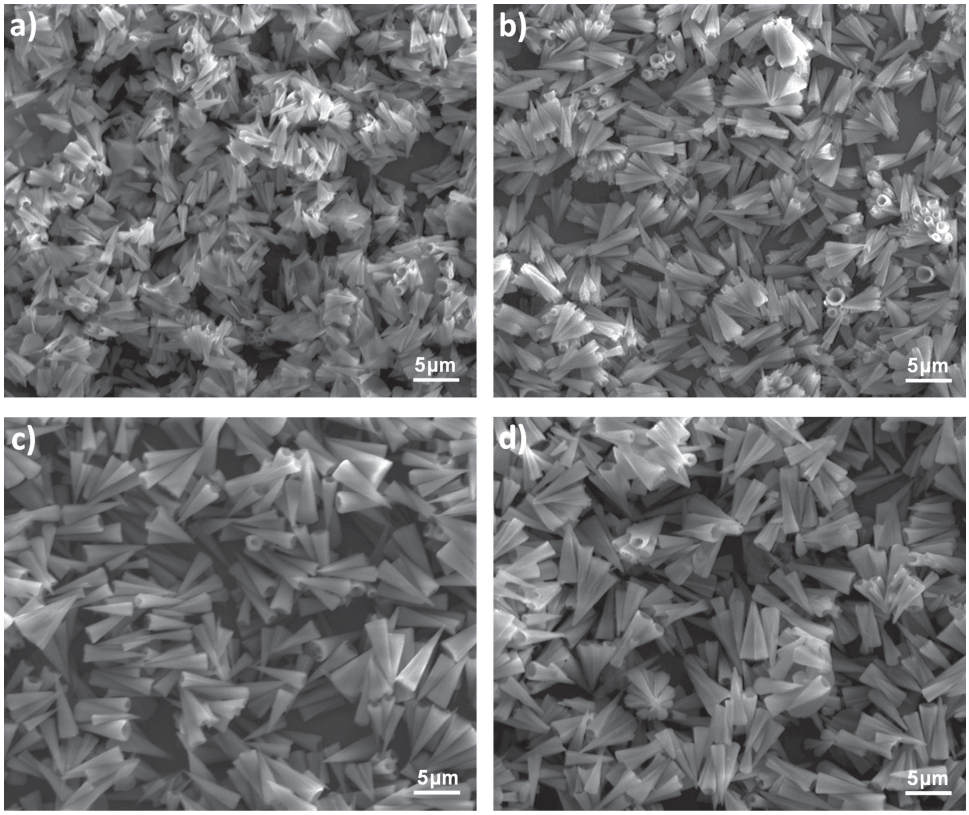

Figure 3. SEM images of layered cobalt hydroxide NCs obtained under different conditions: a) 100 °C, 2 h, b) 100 °C, 4 h, c) 100 °C, 12 h, d) 120 °C, 8 h.

correspondingly increased to 3.5–4.5 μm, 200–300 nm, and 600–800 nm, respectively. We speculate that the NCs appear to form through a rolling-up process of lamellar hydroxides, which is consistent with our previous reports.[3] The length was further elongated to 7.5 μm for NCs obtained from a reaction time of 12 h (Figure 3c). This suggests both the elongation in length and the expansion in diameter with increasing reaction time. It was also discovered that the elevation of temperature was helpful to speed up the reaction. For example, the average length of NCs obtained at 120 °C for 8 h was estimated to be 7 μm (Figure 3d), comparable to that of NCs obtained at 100 °C for 12 h. Nevertheless, it is noteworthy that if the reaction time or temperature was further extended, some impurities might be produced, which appears to be related with the possible oxidation of Co (II) to Co (III).

Surfactant SDS seemed to play a crucial role in the formation of such a peculiar conical feature. Hexagonal cobalt hydroxide platelets, several micrometers in width and several tens of nanometers in thickness, were synthesized without using the surfactant SDS. The product appeared pink in color and was identified as brucite-like β-$Co(OH)_2$ with lattice constants of $a = 0.318$ and $c = 0.465$ nm (Supporting Information, Figure S1a(i),b). On the other hand, if the amount of SDS was increased to 25 mmol, the product turned into a green color same with NCs, also identified as DS^-–intercalated α-type cobalt hydroxide. However, the majority of the product instead consisted of lamellar or platy objects. Only a small portion of NCs with average length of about 1.5 μm was discerned (Supporting Information, Figure S1a(ii),c). The interlayer distance of the lamellar structure can be expanded by increasing the amount of SDS, which may affect the product morphology. Furthermore, inert gas protection was also found crucial in the formation of the NCs. Without a gas protection, DS^-–intercalated cobalt hydroxide product with irregular morphology was obtained (Supporting Information, Figure S1a(iii),d). Based on above experimental observations, an appropriate amount of surfactant SDS and suitable inert gas protection may be considered as required conditions for the synthesis of NCs.

2.2. Exfoliation of Layered Cobalt Hydroxide NCs

Layered metal hydroxides, including NCs, have been usually exfoliated via mechanical shaking in formamide.[3,4,6] In the current study, an alternative procedure, heat treating layered cobalt hydroxide NCs in a formamide-water binary solution, was proposed and performed. The conditions are supposed to be milder than mechanical shaking and would bring new insights into their exfoliation behavior. **Figure 4**a–e depicts the morphological change of NCs during the treatment. After heat treatment for 2 h, the wall thickness generally became thinner than those of original NCs. In particular, some outer layers were observed to unravel from the NC as visualized by a typical TEM observation in Figure 4a. The corresponding magnified part shown in Figure 4b clearly identifies such a detachment effect of some outer layers. Figure 4c depicts a high-resolution TEM (HRTEM) image of the tip part, indicating that the interlayer spacing of the unexfoliated part is kept at 2.4 nm. As displayed in Figure 4d, prolonging the treatment time to 4 h made the unravelling and detaching effect more obvious. Ultimately, these NCs could be completely exfoliated/delaminated into unilamellar nanosheets after a treatment time of 8 h. A typical TEM image of the exfoliated nanosheets is given in Figure 4e. A faint and homogeneous contrast indicates the ultrathin and uniform thickness. A tapping-mode atomic force microscope (AFM) image shown in Figure 4f also discerns ultrathin sheet-like objects with lateral size of several hundred nanometers on the Si wafer. The ultrathin nanosheets are irregular in morphology, indicating possible breakage or fracture of the NCs during the delamination process. The thickness of the nanosheets was measured to be approximately 1.0 nm, which is close to the crystallographic thickness of the host layer of α-type cobalt hydroxide, a clear proof supporting the unilamellar nature.[3,6]

The above characterizations validated that heat treatment in the formamide/water media was also effective in delaminating these NCs, providing an alternative route to the access of unilamellar hydroxide nanosheets. More intriguingly, the identification of such a novel unravelling/unzipping scenario of NCs for the first time is vital in understanding the transformation/evolution of a tubular structure, as well as providing new insights into the exfoliation mechanism of layered hydroxides in general.

2.3. Structural Modification and Phase Transformation

The DS^-–intercalated α-type cobalt hydroxide NCs could be readily exchanged into other inorganic and organic anionic forms by a conventional ion-exchange procedure at room temperature. **Figure 5** depicts XRD patterns of as-prepared products after exchange with Cl^-, ClO_4^-, CH_3COO^-, and NO_3^- anions. The basal diffraction peak, 2.4 nm for the original DS^-–intercalated NCs, shifted to 0.78 nm for Cl^-, 0.91 nm for ClO_4^-, 0.92 nm for CH_3COO^-, and 0.79 nm for NO_3^-–exchanged NCs, respectively. The in-plane diffraction peaks of 100 and 110 retained their original positions, indicating that the host layers are basically intact. After anion-exchange, the conical features with hollow interiors are still apparent (see Supporting Information, Figure S2). On the other hand, the wall thickness of the exchanged products has been significantly reduced in contrast with that of DS^-–intercalated NCs, which is due to the decrease of the interlayer spacing, in good consistency with the XRD results.

As shown in **Figure 6**, the exchange of DS^-–intercalated cobalt hydroxide NCs into other anionic forms were further confirmed by Fourier transform infrared (FT-IR) spectroscopy. In all spectra, broad band at around 3500 cm^{-1} is attributable to the stretching vibration of O–H bonds, which indicates the presence of hydroxyl groups with hydrogen bonding and interlayer water molecules. The weak bands at around 1620–1635 cm^{-1} are well-known as the bending mode of the water molecules.[7] The absorption bands at low-frequency regions, below 635 cm^{-1}, are ascribed to Co–O stretching and Co–OH bending vibrations in the host layers.[8] Besides these common bands, in DS^-–intercalated NCs (spectrum a), the sharp bands at 2915 and 2853 cm^{-1} are characteristic of the asymmetric and symmetric CH_2 stretching vibrations in the alkyl chain of dodecylsulfate,

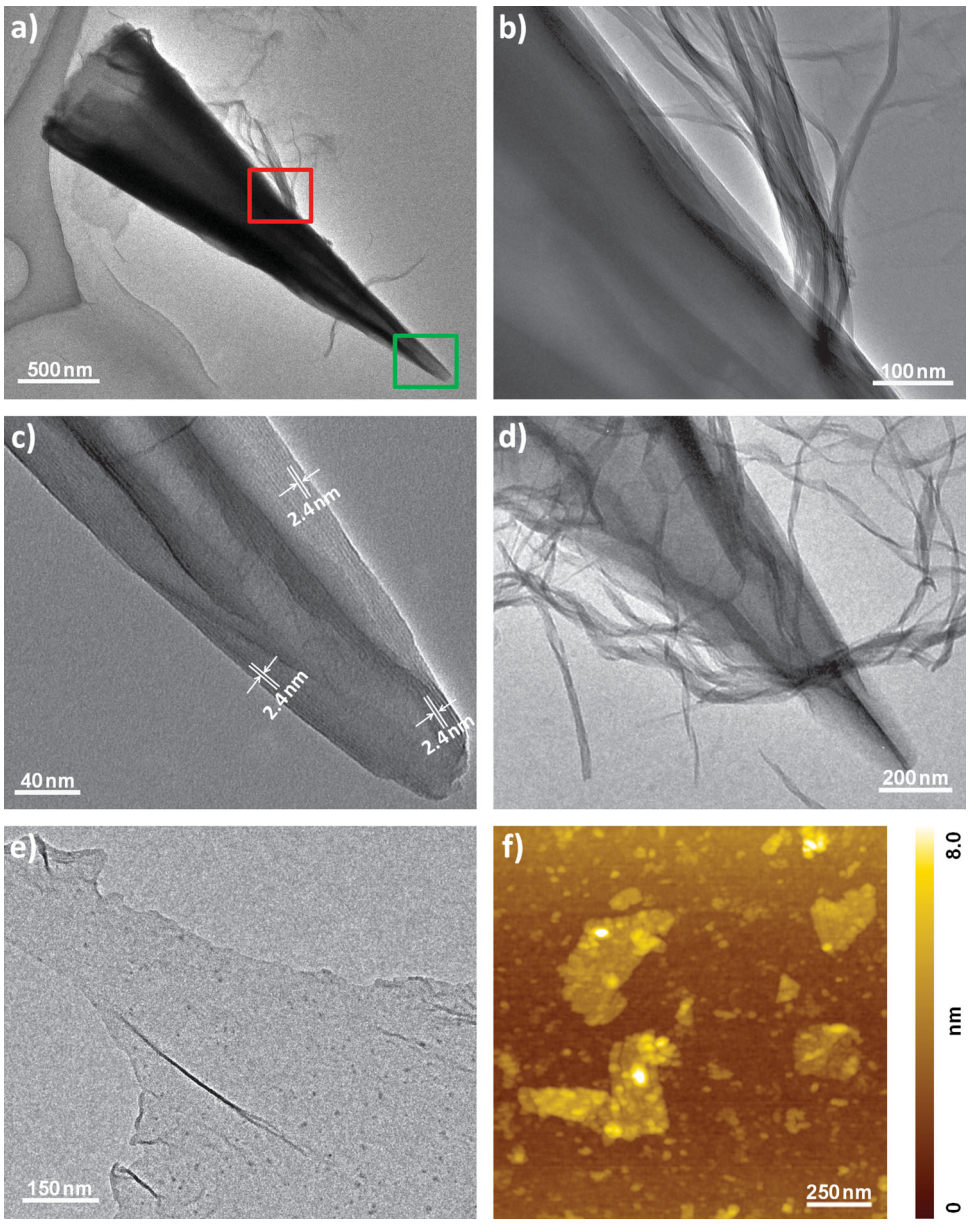

Figure 4. Identification of possible unravelling/unzipping stages of layered cobalt hydroxide NCs. a) Typical TEM image of an individual NC after heat treatment for 2 h. b,c) High-magnification TEM images obtained from the different selected areas of a) corresponding to outer wall part (red box) and tip part (green box), respectively. d,e) Typical TEM images of NC after heat treatment for 4 h and 8 h, respectively. f) Tapping-mode AFM image of the exfoliated nanosheets deposited on Si substrate.

respectively, whereas the weak band at 2959 cm^{-1} is assigned to the stretching vibration of CH_3 group. The band at 1471 cm^{-1} corresponds to the CH_2 bending (scissor) mode whereas those in the range of 1300–900 cm^{-1} are associated with the stretching modes of sulfate group.[9] These features disappeared after the exchange into Cl^- form (spectrum (b)). An additional weak band in spectrum (c) at 1126 cm^{-1} is derived from the exchanged perchlorate anions.[10] In spectrum (d), the bands at 1579 and 1418 cm^{-1} are derived from the symmetric and asymmetric COO^- stretches, respectively, indicating the successful intercalation of acetate groups.[11] Similarly, a sharp and strong absorption band at 1394 cm^{-1} discerned in spectrum (e) is due to the $\nu 3$ vibration mode of nitrate anions.[9,12] These evidences unambiguously confirmed that the cobalt hydroxide NCs possess a high anion exchangeability, desirable for versatile modification of interlayer contents as well as gallery spacing.

The intercalation of different anions might bring an impact to the phase transformation of the hydroxide NCs. The thermal decomposition behaviors of DS^-– and NO_3^-–intercalated NCs were investigated with thermogravimetric (TG) analysis in air in the temperature range of 25–900 °C, as compared in **Figure 7**. In both curves, the gradual mass loss below 100 °C corresponds to the evaporation of the adsorbed water on the surface. The consecutive stages of weight loss in the range 100–170 °C can

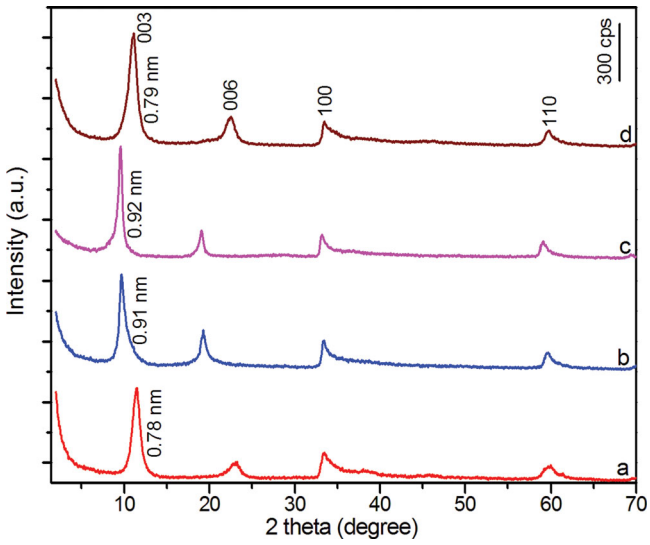

Figure 5. XRD patterns of layered cobalt hydroxide NCs exchanged with various anions: a) Cl^-, b) ClO_4^-, c) CH_3COO^-, d) NO_3^-.

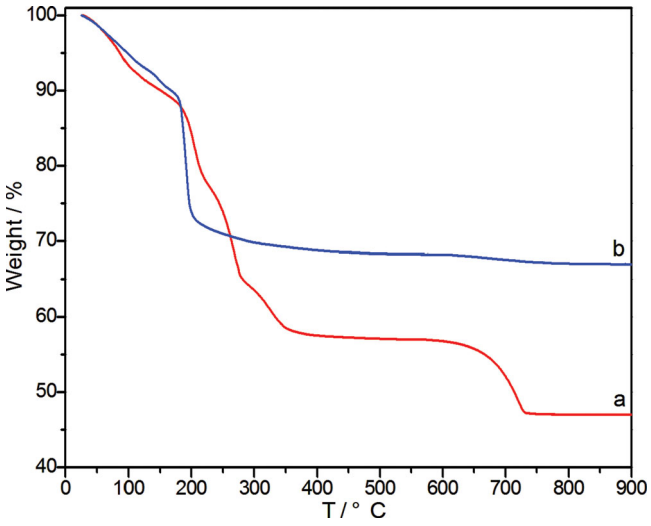

Figure 7. TG curves of layered cobalt hydroxide NCs intercalating a) DS^- and b) NO_3^- anions recorded at a heating rate of 1 °C min^{-1} in air.

be attributed to the removal of interlayer water molecules. After that, the decomposition behavior becomes different. The weight-loss profile of DS^-–intercalated cobalt hydroxide NCs exhibits a major decrease between 170 and 800 °C, which can be mainly attributed to the combustion of DS and dehydroxylation. The combustion of organic components in the DS group led to the formation of cobalt sulfate ($CoSO_4$) as a side product, which was further converted into Co_3O_4 at 800 °C. Such a phase evolution was confirmed by XRD characterizations on calcined products detailed in **Figure 8**.

On the other hand, NO_3^-–intercalated cobalt hydroxide NCs was completely converted into Co_3O_4 at a temperature as low as 400 °C in air. **Figure 9**a shows a typical XRD pattern of the product calcined in air. All of the reflections can be indexed as a pure face-centered cubic phase of spinel Co_3O_4 with lattice constant a =0.808 nm (JCPDS 43–1003). That is to say, the exchange into an NO_3^-–intercalated form is more desirable for the phase transformation into cobalt oxides. In addition, CoO could be selectively obtained by calcination of NO_3^-–intercalated NCs at 400 °C for 2 h under nitrogen flow. The XRD pattern of the converted product is compared in Figure 9b, which can be readily indexed as a cubic structure with lattice constant a =0.426 nm, in good agreement with the standard data for CoO (JCPDS 65–2902). In both patterns, no impurity peak was recognized, indicating a complete conversion into corresponding oxides.

More importantly, as-transformed cobalt oxides (Co_3O_4 and CoO) could retain the original conical framework with hollow interiors. **Figure 10**a,b depicts typical SEM images of the Co_3O_4 product obtained by calcination of NO_3^-–intercalated cobalt

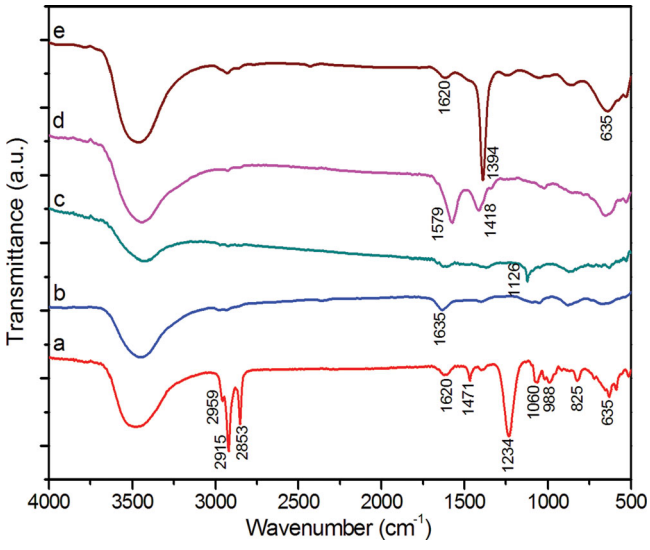

Figure 6. FT-IR spectra of layered cobalt hydroxide NCs exchanged with various anions: a) DS^-; b) Cl^-, c) ClO_4^-, d) CH_3COO^-, e) NO_3^-.

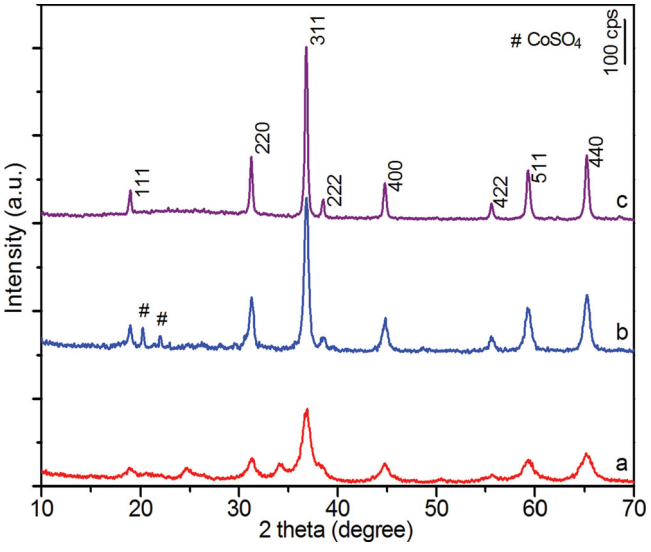

Figure 8. The evolution of XRD patterns of the products obtained by calcination of DS^-–intercalated cobalt hydroxide NCs at a) 400, b) 600, and c) 800 °C for 2 h in air.

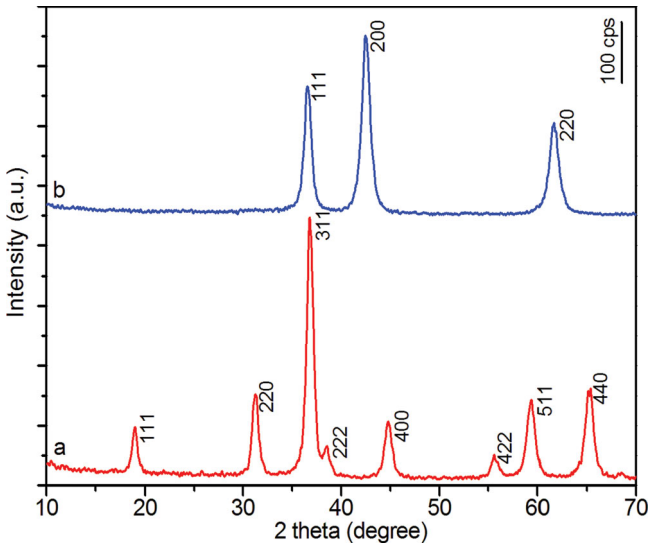

Figure 9. XRD patterns of the products obtained by calcination of NO_3^-–intercalated cobalt hydroxide NCs at 400 °C for 2 h a) in air and b) under nitrogen protection.

hydroxide NCs at 400 °C in air. It is clearly seen that the conical structures as well as hollow interiors are still obvious. Nevertheless, the surfaces of as-calcined Co_3O_4 NCs become wrinkled, which is different from the smooth surface feature of the starting hydroxide NCs. The average length of Co_3O_4 NCs was estimated to be about 4 μm, smaller than that of NO_3^-–intercalated NCs before calcination, implying the tendency to shrink during calcination. A typical TEM image of Co_3O_4 NCs is shown in Figure 10c. In the inset, an SAED pattern was well indexed to spinel Co_3O_4, revealing a polycrystalline nature of the calcined NCs. This indicates the collapse of the layered structure and recrystallization into oxides during calcination. Lattice fringes resolved in the corresponding HRTEM image in Figure 10d were measured to be about 0.24 and 0.20 nm, which are consistent with the interplanar spacings between {311} and {400} in spinel Co_3O_4, respectively. In comparison, a typical SEM image of CoO NCs, obtained by calcination of NO_3^-–intercalated cobalt hydroxide NCs at 400 °C under nitrogen protection, is shown in Figure 10e. Again, the calcined product retained the conical feature with a hollow interior. The hollow nature is also clearly revealed by TEM observation of an individual CoO NC in Figure 10f. The upper inset displays the corresponding SAED pattern, which can be indexed to cubic CoO. Similar to the Co_3O_4 case, as-transformed CoO NCs are also polycrystalline. The lattice spacing in the HRTEM image shown in lower inset of Figure 10f was measured to be about 0.21 nm, agreeing well with the interplanar spacings of {200} for cubic CoO.

2.4. Electrochemical Properties of Cobalt Hydroxide NCs

The electrochemical behavior of cobalt hydroxide NCs and exfoliated nanosheets in 1 M KOH aqueous electrolyte were investigated using cyclic voltammetry (CV) and galvanic charge-discharge cycling. Typical CV curves of layered cobalt hydroxide NCs intercalated with different anions in a potential range of –0.2 to 0.4 V (vs Ag/AgCl) at a scan rate of 10 mV s^{-1} are compared in **Figure 11**a. Two pairs of redox peaks are commonly observed, revealing that there are two quasi-reversible electron-transfer processes, which are directly related with the following Faradaic reactions: $Co(OH)_2 + OH^- \Leftrightarrow CoOOH + H_2O + e^-$ and $CoOOH + OH^- \Leftrightarrow CoO_2 + H_2O + e^-$, respectively.[13] It is well known that the anodic peaks result from the oxidation of $Co(OH)_2$ to CoOOH (≈0.05 V) as well as CoOOH to CoO_2 (≈0.3 V), whereas the cathodic peaks correspond to the reverse reduction process. In comparison with DS^-–intercalated NCs, the redox current was enhanced to some extent after exchange into Cl^- and NO_3^-. It is noteworthy that redox peaks of β-$Co(OH)_2$ hexagonal platelets are the weakest, revealing a poor electrochemical performance. Generally, the Faradaic pseudocapacitance is mainly based on redox reactions at the interface between the active material and the electrolyte. Based on the experimental results, we assume that the interlayer distance and the intercalated anions impart substantial effect on the electrochemical activity of layered transition-metal hydroxides, suggesting a suitable combination of interlayer spacing and anionic species may be required for achieving optimum electrochemical performance. Figure 11b exhibits the galvanostatic charge-discharge curves measured in the potential range between 0 and 0.4 V at a current density of 10 A g^{-1}. The specific capacitance could be calculated from the galvanostatic charge-discharge curves using the equation: $C = I\Delta t/m\Delta V$, where I is charge-discharge current, Δt is the time for a full discharge, m indicates the mass of the active material, and ΔV represents the voltage change after a full discharge.[14] The specific capacitance of layered cobalt hydroxide NCs intercalated with DS^-, Cl^-, and NO_3^- anions was estimated to be approximately 340, 590, and 430 F g^{-1}, while that for cobalt hydroxide nanosheets and β-$Co(OH)_2$ hexagonal platelets was 450 and 260 F g^{-1}, respectively. The capacitances are roughly close to our previously reported value (≈490 F g^{-1}) of layered cobalt hydroxide NCs synthesized under microwave-assisted conditions.[3b] It is generally assumed that the specific capacitances of layered hydroxides will be enhanced with the expansion of interlayer spacing for ion diffusion.[13b]Such an effect was verified by the result that the specific capacitance of β-$Co(OH)_2$ hexagonal platelets is the lowest among all the products. β-$Co(OH)_2$ is composed of neutral host layers without gallery space for anions, which may hinder ion diffusion of electrolyte. However, compared with DS^-– and NO_3^-–intercalated cobalt hydroxide NCs, the Cl^-–intercalated form exhibited the highest specific capacitance. The reason is not clear yet, but it probably originates from the exchange and transport behavior of interlayer OH^- associated with different anionic species, which has been reported for layered α-type cobalt or nickel hydroxides.[15]

2.5. Magnetic Properties of Cobalt Oxide NCs

The magnetic properties of as-transformed cobalt oxide NCs were measured on a superconducting quantum interference device (SQUID). The temperature dependences of the magnetic susceptibility (χ) for Co_3O_4 and CoO NCs under an

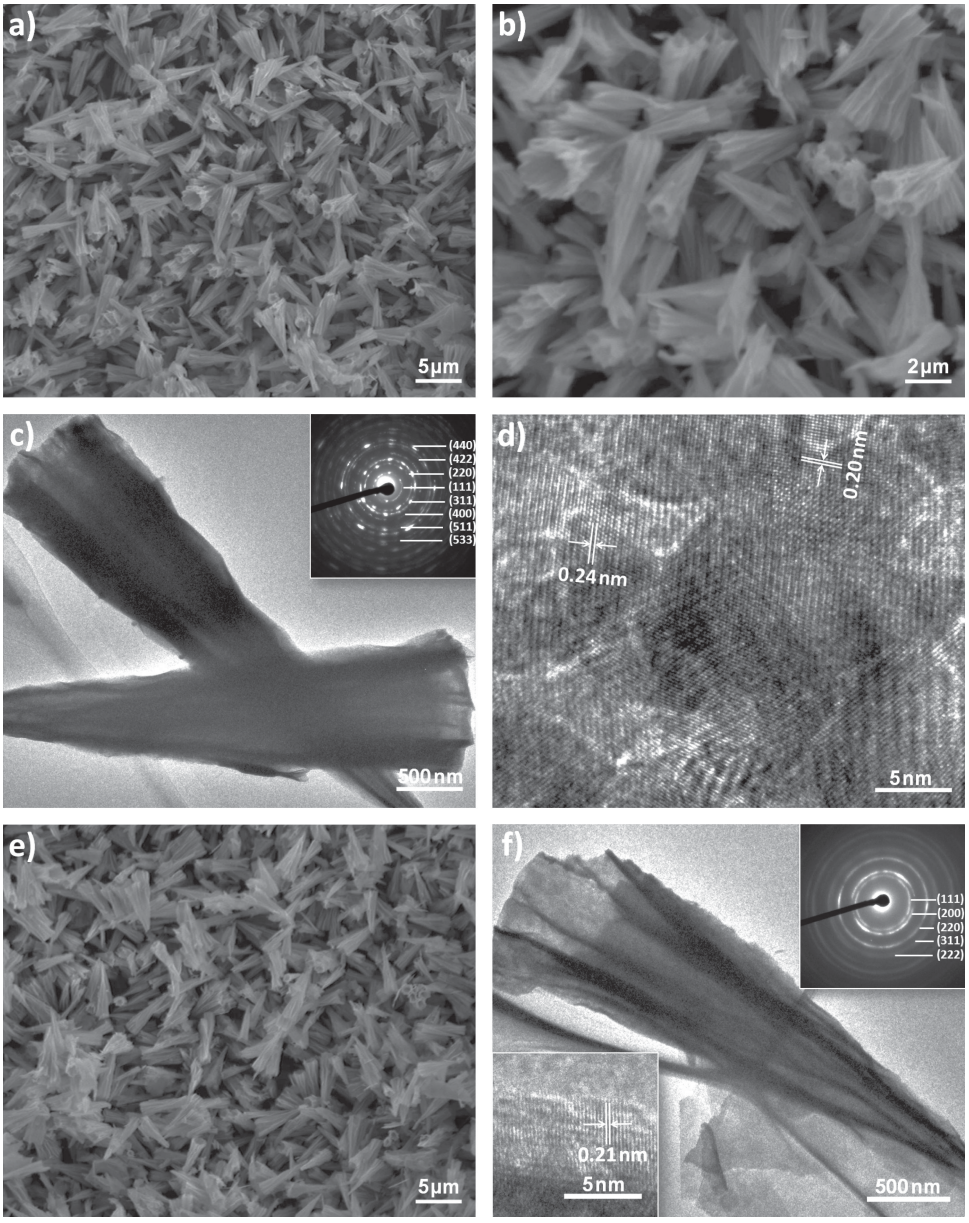

Figure 10. Characterizations of cobalt oxide NCs. a,b) SEM and c) TEM images of Co_3O_4 NCs calcined at 400 °C in air. d) HRTEM image with lattice fringes resolved. e) SEM and f) TEM images of CoO NCs calcined at 400 °C under nitrogen protection. The insets in (c,f) show SAED patterns indexed to be Co_3O_4 and CoO, respectively.

applied field of 500 Oe are provided in **Figure 12**a,b, respectively. Both products exhibited antiferromagnetic transitions at low temperature. For Co_3O_4, the transition occurs at ≈29 K (Néel temperature, T_N), which is lower than that of bulk Co_3O_4 (40 K).[16] In addition to the antiferromagnetic transition, an upturn in the zero-field-cooled (ZFC) curve below T_N is also visible, possibly due to spin canting or other spin scattering effect. The antiferromagnetic transition for CoO NCs takes place at around 70 K, being far lower than the Néel temperature of bulk CoO that is known at about 300 K. The lowering of Néel temperature possibly resulted from the size, shape and surface effects of cobalt oxide NCs, that is, the geometric confinement effect.[17] In order to further analyze the magnetic properties, the Curie-Weiss law was applied to the paramagnetic part, as illustrated by the corresponding insets. The analytical formula was $\chi(T) = N_A\mu^2_{eff}/3k_B(T - \Theta_W)$, where N_A is the Avogadro constant, μ_{eff} is the effective magnetic moment, k_B is Boltzmann's constant and Θ_W is the Weiss temperature. The plots yielded values of Θ_W at –107 K and –406 K for Co_3O_4 and CoO NCs, respectively, suggesting weak antiferromagnetic interaction in Co_3O_4 while a very strong one in CoO NCs. The hysteresis loops for Co_3O_4 and CoO NCs at 2 and 300 K are depicted in Figure 12c,d, respectively. The almost linear relation between the magnetization and magnetic field for Co_3O_4 at 2 and 300 K again demonstrates that the product has an antiferromagnetic ground state. For CoO NCs, despite that

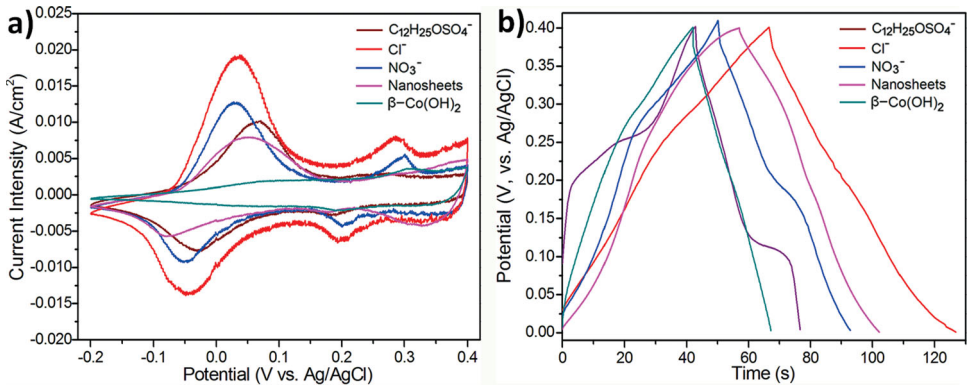

Figure 11. Electrochemical characterizations of a) layered cobalt hydroxide NCs intercalated with various anions, unilamellar cobalt hydroxide nanosheets, and β-$Co(OH)_2$ hexagonal platelets. b) Galvanostatic charge-discharge curves at a current density of 10 A g^{-1}.

the data at low temperature range reflect a slight curvature, the magnetization curves as a whole are nearly linear without forming clear hysteresis loops, also indicative of an antiferromagnetic ground state. Because of the peculiar morphological and structural characteristics, as well as finite size effect of cobalt oxide NCs, the magnetic properties are considerably different from those found in their bulk oxide counterparts, which might anticipate some prospective applications in magneto-optical or magnetic recording devices, etc.

3. Conclusions

In summary, a convenient and reliable synthetic strategy was presented for the preparation of DS^-–intercalated cobalt hydroxide NCs in large quantities based on urea hydrolysis in oil bath. The NCs could be gradually unwrapped/exfoliated into unilamellar nanosheets in the formamide-water binary solution through heat treatment. Meanwhile, DS^-–intercalated cobalt hydroxide NCs could be easily modified into various

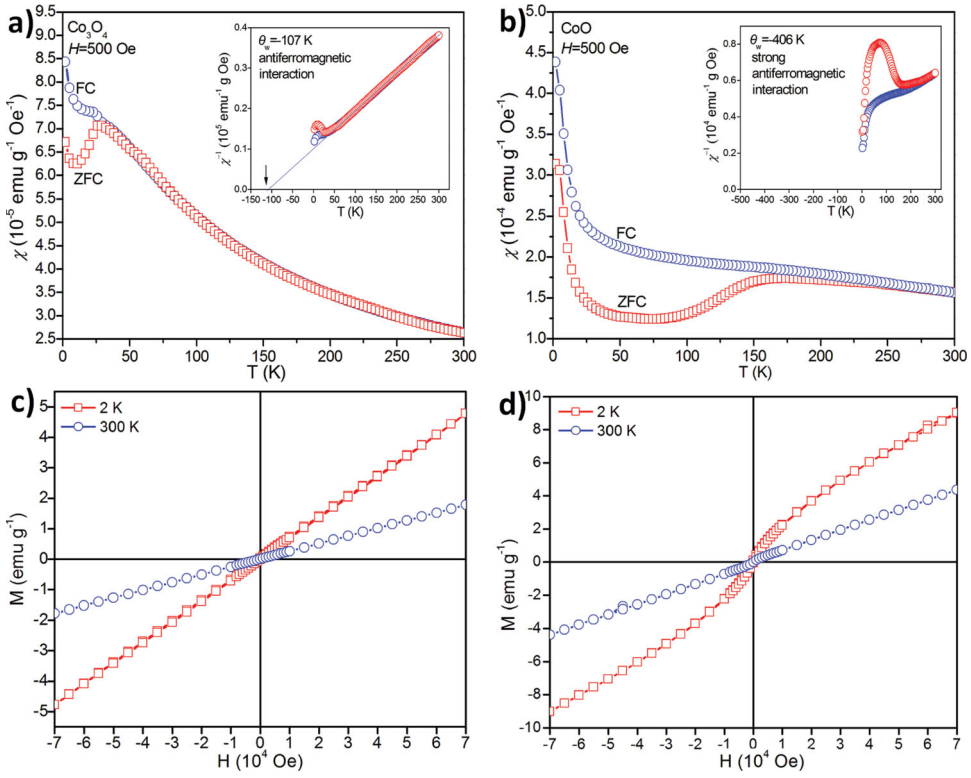

Figure 12. Temperature dependence of magnetic susceptibility (χ) for a) Co_3O_4 and b) CoO NCs measured under an applied field of 500 Oe. The insets in a) and b) illustrate the corresponding plots of inverse susceptibility (χ^{-1}) vs temperature. Isothermal magnetization curves for c) Co_3O_4 and d) CoO NCs at 2 and 300 K, respectively.

inorganic or organic anionic forms via an anion-exchange process at ambient temperature. The anion-exchanged products exhibited different oxidation behavior. Particularly, NO_3^-–intercalated NCs could be more readily calcined into cobalt oxides (e.g., Co_3O_4 and CoO) retaining original conical features in comparison with the DS^-–intercalated form. The electrochemical characterizations suggested that a suitable combination of interlayer gallery space and intercalated anions was required for achieving optimum electrochemical performance. The magnetic measurements revealed both antiferromagnetic properties of calcined Co_3O_4 and CoO NCs, but the Néel temperature values were lower than those of their bulk counterpart materials. The versatile structural modification of layered cobalt hydroxide NCs and their derivatives are expected to bring new opportunities for further fundamental research, as well as for technological applications in electrochemical energy storage or magneto-optical devices.

4. Experimental Section

All chemicals of analytical grade were purchased from Wako Chemical Reagents Company (Japan). They were used without further purification. Milli-Q water was used throughout the experiments.

Synthesis of Layered Hydroxide NCs: In a typical synthesis, $CoCl_2{\cdot}6H_2O$ (99.5%, 5 mmol), urea (99.0%, 35 mmol), and SDS (98.0%, 0–25 mmol) were charged into a three-neck flask and dissolved in 500 cm^3 Milli-Q water to give the final concentrations of 10, 70, and 0–50 mM, respectively. The pH of the initial mixture was about 7. The flask was then placed in an oil bath and heated at 100–120 °C for 2–12 h under continuous magnetic stirring and a nitrogen gas protection. The resulting product was filtered, washed with Milli-Q water and absolute ethanol, and finally dried in air at 60 °C for 4 h. The yield of NCs was estimated as ~90% based on the calculation of cobalt source.

Exfoliation of Layered Cobalt Hydroxide NCs: Layered cobalt hydroxide NCs (0.2 g) were dispersed in a formamide-water binary solution (500 cm^3, 1:4 v/v), which was then heated at 80 °C for 1–8 h under continuous magnetic stirring and a nitrogen gas protection. The resulting translucent colloidal suspension was further treated by centrifugation at 4 000 rpm for 20 min to remove possible unexfoliated NCs.

Anion Exchange and Calcination of Layered Cobalt Hydroxide NCs: Layered cobalt hydroxide NCs intercalated with various anions were prepared by an ethanol-assisted anion-exchange approach. For instance, as-prepared DS^-–intercalated NCs (0.2 g) were dispersed into an ethanol-water binary solution (200 cm^3, 1:1 v/v) of 1 M $NaNO_3$, NaCl, $NaClO_4$, or $NaCOOCH_3$ in a flask, respectively. After being purged with nitrogen gas, the flask was tightly capped and mechanically shaken for 48 h at room temperature. The product was filtered, washed with anhydrous ethanol and finally dried in air at 60 °C for 4 h. DS^-–intercalated cobalt hydroxide NCs and corresponding NO_3^-–exchanged products were calcined in air or under nitrogen protection to prepare Co_3O_4 or CoO NCs at 400 or 800 °C for 2 h, respectively.

Characterizations: XRD data were recorded on a Rigaku Rint-2200 diffractometer with a monochromatic Cu Kα radiation ($\lambda = 0.15405$ nm). The morphologies and dimensions of the as-prepared products were examined with a Keyence VE8800 scanning electron microscope. TEM characterizations were performed on a JEOL JEM-3000F transmission microscope. A Seiko SPA 400 atomic force microscope was used to examine the topography of the nanosheets deposited on Si wafers. A cleaned Si wafer was immersed in the colloidal formamide-water suspension for 20 min, which was followed by rinsing with a copious amount of water and drying under a N_2 stream. AFM images were acquired in tapping mode using a Si tip cantilever with a force constant of ≈20 N m^{-1}. FT-IR spectra were recorded using the KBr pellet method on a Varian 7000e FT-IR spectrophotometer equipped with a liquid-nitrogen-cooled Mercury-Cadmium-Telluride (MCT) detector. Thermogravimetric and differential thermal analyses (TG-DTA) were carried out using a Rigaku TGA-8120 instrument in a temperature range of 25–900 °C at a heating rate of 1 °C min^{-1} under an air flow. Cyclic voltammetry and galvanic charge-discharge measurements were carried out on a Solartron electrochemistry workstation using a three electrode cell with 1 M KOH as the electrolyte, a Ag/AgCl electrode as reference electrode, and platinum wire as counter electrode, respectively. For electrochemical measurements, ≈1 mg of hydroxide NCs or nanosheets deposited on graphite foils were used as working electrodes. The working electrodes were prepared as follows: 80 wt% of as-prepared NCs or nanosheets was mixed with 10 wt% of acetylene black (>99.9%) and 10 wt% of polytetrafluoroethylene (PTFE, >99.9%) in an agate mortar until a homogeneous black powder was obtained. Then a few drops of ethanol were added. After briefly allowing the ethanol to evaporate, the suspension was dropped on a 1 cm × 1 cm graphite foil. The electrode was dried at 80 °C for 12 h in air and then was pressed under 40 MPa before electrochemical measurements. Magnetic measurements were conducted using a Quantum Design MPMS XP-5 superconducting quantum interference device (SQUID).

Supporting Information

Supporting Information is available from the Wiley Online Library or from the author.

Acknowledgements

The authors acknowledge the financial support by CREST of the Japan Science and Technology Agency (JST), the World Premier International Center Initiative (WPI) on Materials Nanoarchitectonics, MEXT, Japan. R.M. acknowledges support from JSPS KAKENNHI Grant number 24310095. X.L. acknowledges support from National Natural Science Foundation of China (51372279), Hunan Provincial Natural Science Foundation of China (13JJ1005), and Shenghua Scholar Program of Central South University.

Received: January 20, 2014
Revised: February 20, 2014
Published online: April 4, 2014

[1] a) D. L. Bish, *Bull. Mineral.* **1980**, *103*, 170; b) M. Ogawa, K. Kuroda, *Chem. Rev.* **1995**, *95*, 399; c) B. Sels, D. De Vos, M. Buntinx, F. Pierard, A. Kirsch-De Mesmaeker, P. Jacobs, *Nature* **1999**, *400*, 855; d) B. F. Sels, D. E. De Vos, P. A. Jacobs, *Catal. Rev.* **2001**, *43*, 443; e) B. M. Choudary, S. Madhi, N. S. Chowdari, M. L. Kantam, B. Sreedhar, *J. Am. Chem. Soc.* **2002**, *124*, 14127; f) S. Tezuka, R. Chitrakar, A. Sonoda, K. Ooi, T. Tomida, *Green Chem.* **2004**, *6*, 104; g) G. R. Williams, D. O'Hare, *J. Mater. Chem.* **2006**, *16*, 3065; h) J.-H. Yang, Y.-S. Han, M. Park, T. Park, S.-J. Hwang, J.-H. Choy, *Chem. Mater.* **2007**, *19*, 2679; i) P. J. Sideris, U. G. Nielsen, Z. Gan, C. P. Grey, *Science* **2008**, *321*, 113; j) T.-Y. Wei, C.-H. Chen, H.-C. Chien, S.-Y. Lu C.-C.Hu, *Adv. Mater.* **2010**, *22*, 347.

[2] a) Y. Zhao, F. Li, R. Zhang, D. G. Evans, X. Duan, *Chem. Mater.* **2002**, *14*, 4286; b) Z. Liu, R. Ma, M. Osada, K. Takada, T. Sasaki, *J. Am. Chem. Soc.* **2005**, *127*, 13869; c) Y. Han, Z.-H. Liu, Z. Yang, Z. Wang, X. Tang, T. Wang, L. Fan, K. Ooi, *Chem. Mater.* **2008**, *20*, 360; d) S. Ida, D. Shiga, M. Koinuma, Y. Matsumoto, *J. Am. Chem. Soc.* **2008**, *130*, 14038.

[3] a) X. H. Liu, R. Ma, Y. Bando, T. Sasaki, *Angew. Chem. Int. Ed.* **2010**, *49*, 8253; b) X. H. Liu, R. Ma, Y. Bando, T. Sasaki, *Adv. Mater.* **2012**, *24*, 2148.

[4] a) P. S. Braterman, Z. P. Xu, F. Yarberry, in *Layered Double Hydroxides (LDHs), Handbook of Layered Materials*, (Eds: S. M. Auerbach, K. A. Carrado, P. K. Dutta), Marcel Decker, Inc., New York **2004**, p 373; b) Q. Wang, D. O'Hare, *Chem. Rev.* **2012**, *112*, 4124.
[5] a) E. Coronado, C. Marti-Gastaldo, E. Navarro-Moratalla, A. Ribera, S. J. Blundell, P. J. Baker, *Nat. Chem.* **2010**, *2*, 1031; b) R. Ma, T. Sasaki, *Adv. Mater.* **2010**, *22*, 5082; c) D. P. Yan, J. Lu, J. Ma, M. Wei, D. G. Evans, X. Duan, *Angew. Chem. Int. Ed.* **2011**, *50*, 720; d) L. Wang, D. Wang, X. Y. Dong, Z. J. Zhang, X. F. Pei, X. J. Chen, B. Chen, J. Jin, *Chem. Commun.* **2011**, *47*, 3556.
[6] a) Z. Liu, R. Ma, Y. Ebina, N. Iyi, K. Takada, T. Sasaki, *Langmuir* **2007**, *23*, 861; b) R. Ma, K. Takada, K. Fukuda, N. Iyi, Y. Bando, T. Sasaki, *Angew. Chem. Int. Ed.* **2008**, *47*, 86.
[7] a) Z. P. Xu, H. C. Zeng, *Chem. Mater.* **1999**, *11*, 67; b) P. Jeevanandam, Y. Koltypin, Y. Mastai, *J. Mater. Chem.* **2000**, *10*, 511; c) D. H. Sun, J. L. Zhang, H. J. Ren, Z. F. Cui, D. X. Sun, *J. Phys. Chem. C* **2010**, *114*, 12110.
[8] a) Y. Hou, H. Kondoh, M. Shimojo, T. Kogure, T. Ohta, *J. Phys. Chem. B* **2005**, *109*, 19094; b) E. Lima, M. J. Martínez-Ortiz, R. I. G. Reyes, M. Vera, *Inorg. Chem.* **2012**, *51*, 7774.
[9] a) F. X. Geng, H. Xin, Y. Matsushita, R. Ma, M. Tanaka, F. Izumi, N. Iyi, T. Sasaki, *Chem. Eur. J.* **2008**, *14*, 9255; b) T. Gao, B. P. Jelle, *J. Phys. Chem. C* **2013**, *117*, 17294.
[10] R. Ma, Z. Liu, K. Takada, N. Iyi, Y. Bando, T. Sasaki, *J. Am. Chem. Soc.* **2007**, *129*, 5257.
[11] a) L. Poul, N. Jouini, F. Fievet, *Chem. Mater.* **2000**, *12*, 3123; b) L. J. McIntyre, L. K. Jackson, A. M. Fogg, *Chem. Mater.* **2008**, *20*, 335; c) P.-P. Wang, B. Bai, S. Hu, J. Zhuang, X. Wang, *J. Am. Chem. Soc.* **2009**, *131*, 16953.
[12] M. Shao, M. Wei, D. G. Evans, X. Duan, *Chem. Commun.* **2011**, *47*, 3171.
[13] a) L. Cao, F. Xu, Y. Y. Liang, H. L. Li, *Adv. Mater.* **2004**, *16*, 1853; b) L. Wang, Z. H. Dong, Z. G. Wang, F. X. Zhang, J. Jin, *Adv. Funct. Mater.* **2013**, *23*, 2758.
[14] a) H. Wang, H.S. Casalongue, Y. Liang, H. Dai, *J. Am. Chem. Soc.* **2010**, *132*, 7472; b) S. Chen, J. Zhu, X. Wang, *J. Phys. Chem. C* **2010**, *114*, 11829.
[15] a) Z. A. Hu, Y. L. Xie, Y. X. Wang, L. J. Xie, G. R. Fu, X. Q. Jin, Z. Y. Zhang, Y. Y. Yang, H. Y. Wu, *J. Phys. Chem. C* **2009**, *113*, 12502; b) J. W. Lee, J. M. Ko, J.-D. Kim, *J. Phys. Chem. C* **2011**, *115*, 19445.
[16] a) W. L. Roth, *J. Phys. Chem. Solids* **1964**, *25*, 1; b) L. He, C. P. Chen, N. Wang, W. Zhou, L. Guo, *J. Appl. Phys.* **2007**, *102*, 103911.
[17] M. Ghosh, E. V. Sampathkumaran, C. N. R. Rao, *Chem. Mater.* **2005**, *17*, 2348.